Optimization and evaluation of propolis liposomes as a promising therapeutic approach for COVID-19

Hesham Refaat [a], Fatma M. Mady [b], Hatem A. Sarhan [b], Heba S. Rateb [c], Eman Alaaeldin [a,b,*]

[a] *Department of Pharmaceutics, Faculty of Pharmacy, Deraya University, Minia, Egypt*
[b] *Department of Pharmaceutics, Faculty of Pharmacy, Minia University, Minia, Egypt*
[c] *Department of Pharmaceutical Chemistry, College of Pharmaceutical Science and Drug Manufacturing, Misr University for Science and Technology, Cairo, Egypt*

A R T I C L E I N F O

A B S T R A C T

The present work aimed to develop an optimized liposomal formulation for enhancing the anti-viral activity of propolis against COVID-19. Docking studies were performed for certain components of Egyptian Propolis using Avigan, Hydroxychloroquine and Remdesivir as standard antivirals against both COVID-19 3CL-protease and S1 spike protein. Response surface methodology and modified injection method were implemented to maximize the entrapment efficiency and release of the liposomal formulation. The optimized formulation parameters were as follow: LMC of 60 mM, CH% of 20% and DL of 5 mg/ml. At those values the E.E% and released % were 70.112% and 81.801%, respectively with nanosized particles (117 ± 11 nm). Docking studies revealed that Rutin and Caffeic acid phenethyl ester showed the highest affinity to both targets. Results showed a significant inhibitory effect of the optimized liposomal formula of Propolis against COVID-3CL protease (IC50 = 1.183 ± 0.06) compared with the Egyptian propolis extract (IC50 = 2.452 ± 0.11), $P < 0.001$. Interestingly, the inhibition of viral replication of COVID-19 determined by RT_PCR has been significantly enhanced via encapsulation of propolis extract within the liposomal formulation ($P < 0.0001$) and was comparable to the viral inhibitory effect of the potent antiviral (remdesivir). These findings identified the potential of propolis liposomes as a promising treatment approach against COVID-19.

1. Introduction

Coronavirus 19 (COVID-19) is the latest member of the coronavirus family that causes severe acute respiratory syndrome (SARS). However, it possess higher potential of infectivity and transmission than other SARS family members (Liu et al., 2020; Zhu et al., 2020). Although ATP antagonists such as Remdesivir has been theoretically effective against the viral replication via RNA-dependent RNA polymerase (RdRP) inhibition(Gordon et al., 2020), the concomitant general inhibition of other ATP-dependent enzymes like protein kinases and ATPases may result in numerous side effects. Therefore, the effective treatment of corona virus requires selective inhibition of certain host enzyme that is important for the viral replication with minimal effect on other enzymes which may affect the normal physiology of the host. Fortunately, kinase PAK1 is a selective enzyme which is important for malarial and viral infection

(Maruta, 2014). Activation of PAK1 is responsible for viral infection, malarial infection, aging and even cancer (Maruta, 2014).

Propolis or bee glue, a resinous material produced by bees to protect their hives, is rich in wide range of compounds such as flavonoids, polyphenolics, amino acids, resins and oils (Simone-Finstrom and Spivak, 2010). Propolis is well-known for its antibacterial (Kujumgiev et al., 1999), antiviral (Kujumgiev et al., 1999; Kumazawa et al., 2004), anti-inflammatory (Banskota et al., 2001) and immunomodulatory effect (Marcucci, 1995). Rutin, caffeic acid phenethyl ester, Quercetin, p-coumaric acid, benzoic acid, galangin, pinocembrin, chrysin, and Pinobankasin are among the active components responsible for the pharmacological effects of propolis (El Hady and Hegazi, 2002; Tolba et al., 2013; Lan et al., 2016; Badria et al., 2018).

Caffeic acid phenethyl ester (CAPE), the major constituent of the Egyptian propolis, is one of PAK1 inhibitors which acts via the down

---

regulation of RAC (a signaling protein in human cells) (Maruta and He, 2020). In other words, CAPE is capable of blocking viral infection including corona virus and preventing coronavirus-induced lung fibrosis (Maruta, 2014; Maruta and He, 2020).

Another mechanism that may be implicated in the anti-viral effect of propolis against COVID-19 is the improved inhibition potential of propolis components, rutin, myricetin and caffeic acid phenethyl ester , on ACE II receptors (Güler et al., 2020). ACE II has been proven to be strongly recognized by SARS-CoV-2 than SARS CoV (Wan et al., 2020), hence increasing the opportunity to be transmitted from person to person. Therefore, blocking ACE receptors has an essential role in treatment of SARS-CoV-2.

Collecting all those together, essentiates the need for a good delivery system for this promising natural product for the treatment of that pandemic disease. The efficient delivery of propolis may be hindered by the sticky and the resinous nature of the extract. Moreover, a special dosage form is required to deliver both the hydrophilic and the lipophilic contents of propolis extract. Therefore, this study aimed at optimizing a liposomal formulation for the efficient delivery of propolis components. To the best of our knowledge, it is the first study to formulate a nanocarrier dosage form to make the best use of propolis in treatment of COVID-19.

2. Experimental

2.1. Materials

Lipoid S75 (70% phosphatidylcholine-containing fat free soybean phospholipids) was kindly given by lipoid company (Germany). Alcoholic extract of Propolis (PE) was purchased from VACSERA-EGYPT (Cell Culture Department). Cholesterol was obtained from Fluka chemical co. (India). Ethanol (absolute) was obtained from El-Nasr Pharmaceuticals, (Egypt). All chemicals and reagents were of analytical grade and purchased from (Sigma Aldrich).

2.2. Methodology

2.2.1. Molecular docking

In this study, some compounds detected in the ethanolic propolis extracts were used as ligands for COVID-19 3CL-protease (main protease) (PDB ID: 6LU7) (Jin et al., 2020); COVID-19 S1 spike protein subunit (PDB ID: 7BZ5) (Wu et al., 2020); as viral targets in order to evaluate their binding affinities and identify their inhibition activities and binding modes at the active site of each target. The crystal structure of them was downloaded from protein data bank web site. All bound water molecules, ligands and cofactors were removed from the protein. All components were constructed on ChemDraw 3D structures using ChemDraw 3D ultra 9.0 software then they were energetically minimized by using MM2, Jop Type with 100 iterations and minimum RMS gradient of 0.01 and saved as MDL MolFile. Docking studies were performed using Molsoft Internal Coordinate Mechanics (ICM) 3.4-8C program as reported (https://www.rcsb.org/).

2.2.2. Preparation of Propolis-liposomes (PP-Lip) using spraying technique

PP-Lip were prepared by spraying technique reported by *Refaat et al* (Refaat et al., 2019), nevertheless we aimed to modify the formulation parameters to increase the entrapment efficiency and release of the prepared liposomes with maintaining small particle size in the nanoscale. Briefly, propolis, cholesterol and lipid S75 were dissolved in the minimal volume of absolute ethanol then sprayed (40 < ul > L per second stirred at 1500 rpm at 80 °C) on the surface of sucrose-containing distilled water (9% w/v). After evaporation of ethanol by stirring, the spontaneously formed liposomes were kept overnight at 4 °C for optimum annealing of the formed lipid bilayer (Fueldner, 1981). Manual removal of the cooled aggregated free unencapsulated propolis at the surface of the liposomal suspension was carried out.

Table 1
Three selected independent factors and their ranges and levels.

Factors	Codes	Ranges and levels		
		−1	0	1
LMC	A	80	60	40
CH%	B	66	43	20
DL	C	5	3.25	1.5

LMC: lipid molar concentration, CH%: cholesterol percentage, DL: drug loading.

2.2.3. Percentage of entrapment efficiency (%EE) of formulated PP-Lip

The percentage of entrapped content of flavonoids was measured exactly as reported by *Refaat et al* (Refaat et al., 2019). First, free drug was removed by centrifugation of liposomal suspension at 15000 rpm at 4 °C for 2 h. Separated liposomes were washed twice in distilled water to confirm the complete removal of free propolis. Liposomes were decomposed by sonication in absolute alcohol then vortexed to form homogenous suspension which was centrifuged at 15000 rpm for 30 min. The entrapped amount of flavonoids was calculated in 100 μl of the separated supernatant by addition of 100 μl of 10% alcoholic aluminum chloride. The volume was completed to 2 ml using absolute alcohol; then, the absorbance was dignified by a UV/Vis spectrophotometer at 410 nm (Spectronic Genesys®, with Winspec Software, Spectronic, (Pittsford, NY, USA). Blank liposomes were prepared using the same procedure to subtract their absorbance form PP-Lip. The following equation was used to calculate the mean of three repeated values of entrapment percentage of flavonoids: (López-Pinto et al., 2005)

$$E.E\% = \frac{(amount\ of\ flavonoids\ entrapped)}{(total\ amount\ of\ flavonoids\ added)} X100$$

2.2.4. In vitro release study

In vitro release of propolis from the prepared PP-Lip was studied using the semipermeable membrane which was immersed in 0.9% sodium chloride solution one hour before use. Then the membrane was fitted on modified Franz cell with a reservoir compartment containing 20 ml phosphate citrate buffer containing 1% tween 80 (pH 7.4) as a receptor media. Aliquots of PP-Lip formulations with equivalent drug content (1 mg) were added to the sample compartment. The system was shaken in a thermostatic shaker at 37 ± 0.5 °C at 50 ± 10 rpm. Samples of 1 ml of the release medium were withdrawn at predetermined time intervals over a period of 6 h and replaced with the same volume of fresh media maintained at the same temperature. flavonoidal concentration was determined spectrophotometrically at 420 nm according to *woisky and salatino* (Woisky and Salatino, 1998). All these experiments were accomplished in a triplicate manner, the average values were reported, and cumulative percentage of released flavonoids was calculated.

2.2.5. Optimized parameters for the preparation of PP-Lip using response surface methodology

Lipid molar concentration, cholesterol % and flavonoidal loading were the three chosen factors to study their effect on the entrapment efficiency and release of the prepared PP-Lip. The factors were analyzed at three levels, Lipid molar concentration (LMC) (80, 60, 40 mM), cholesterol percentage (CH)% (66, 43, 20%), and drug loading (DL) (5, 3.25, 1.5 mg) (Table 1). The 17 formulations were prepared according to box Behnken design and the response surface diagram was assembled using Design Expert software, version 11 (StatEase®, Minneapolis, MN, USA) and were used to optimize a liposomal formulation of propolis extract.

2.2.6. In vitro 3CL-protease inhibition test

To gain more insight into the effect of both propolis extract and the propolis liposomes on the inhibition of viral RNA 3CL-protease and consequently blocking viral replication, 3CL- Protease (SARS-CoV-2) Assay Kit was used (He et al., 2020). 3CL-protease inhibition was tested for propolis extract, propolis liposomes, solvent of the extract (alcohol)
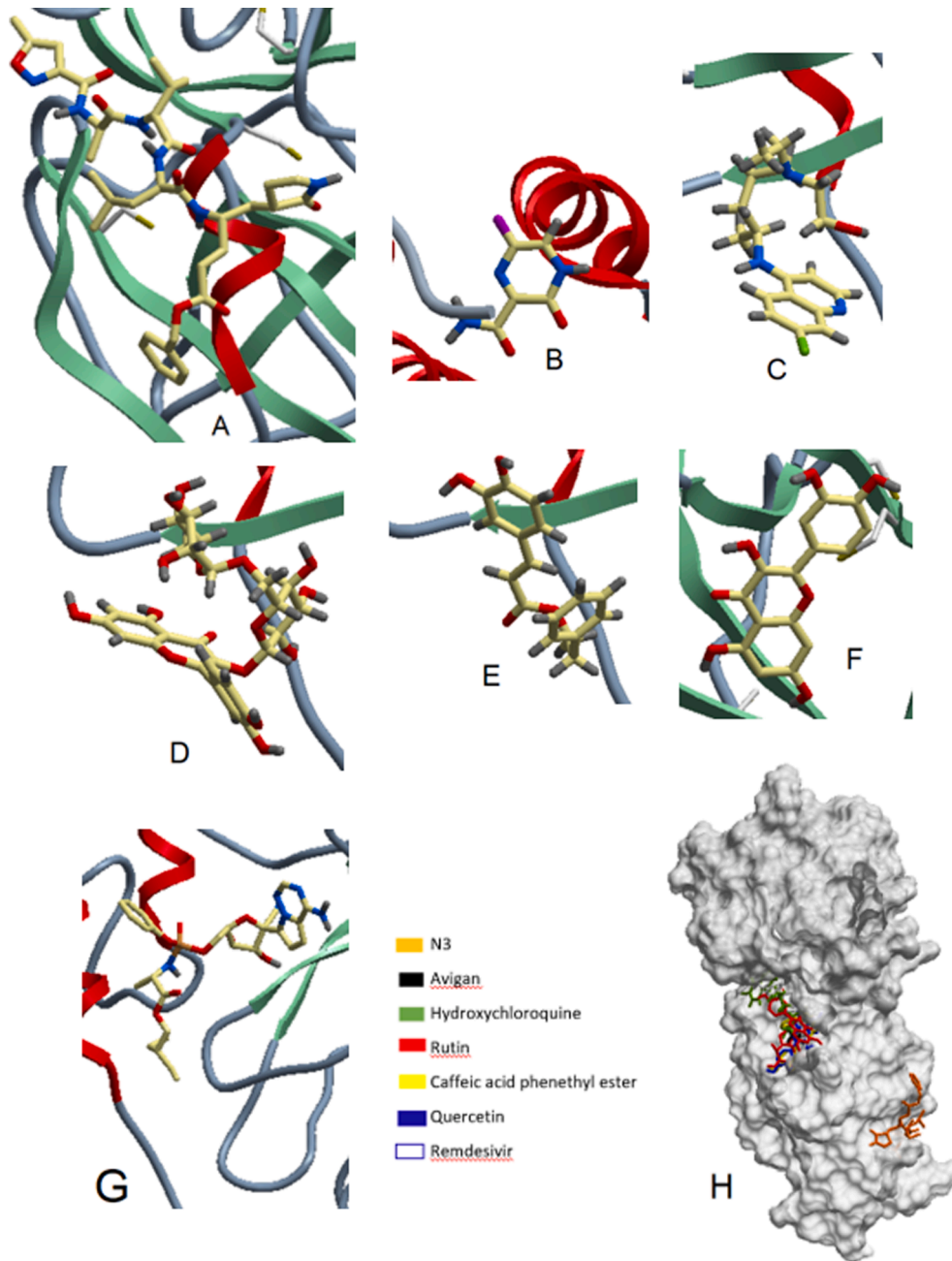
Fig. 1. 3D-plots for docking of A) N3, native ligand; B) Avigan; c) Hydroxychloroquine; D) Rutin; E) Caffeic acid phenethyl ester and F) Quercetin G) Remdesivir in the active site of COVID-19 3CL-protease, (pdb ID: 6LU7). H) 3D-plot for comparison pose docking of native ligand, 2 standards and the most active 3 components of Egyptian propolis.

and Remdesivir as a positive control. 3CL-Protease in Assay buffer was diluted with 1 mM DTT at 3–5 ng/µl (90–150 ng per reaction). Thirty µl diluted 3CL-Protease enzyme solution was added to wells. Ten µl Remdesivir (500 µM) was added to the wells of the positive control. The inhibitor solution was prepared by dilution in 1% DMSO. Ten µl inhibitor solution was added to each well of "Test Sample". Five percentage was added to "Blank" and "Positive Control" wells. 3CL- Protease enzyme was Pre-incubated with the inhibitor solution for 30 min at room temperature with slow shaking. Five mM 3CL-Protease substrate was diluted (1:20) in assay buffer with DTT, to make a 250 µM solution. Reaction was started by adding 10 µl of the substrate solution to each well. Plate was sealed and incubated overnight. fluorescence intensity was measured in a microtiter plate-reading fluorimeter (TECAN spark reader).

2.2.7. Real time PCR for evaluation of anti-viral effect of propolis

To evaluate the antiviral potential of propolis extract and liposomal propolis against corona virus, real time PCR using classical cell culture was adopted (Günther et al., 2004; López-Pinto et al., 2005). Vero cells were seeded in a 24-well plate (4 × 104 /well). After twenty-four hours cells were infected with COVID-19 at a multiplicity of infection (MOI) of 0.01. One hour later, the inoculum was replaced by fresh medium containing predetermined concentrations of test compound (extract solvent (alcohol), lipids, propolis extract, propolis liposomes, Remdesivir as positive control). Percentage of inhibition of COVID-19 replication was determined via estimation of viral RNA concentration using RT-PCR (Drosten et al., 2003). Briefly, A 25-µl reaction was maintained using 5 µl of RNA, 12.5 µl of 2 X reaction buffer solution introduced with the Superscript III one step RT-PCR system accompanied with Platinum Taq Polymerase (Invitrogen; containing 0.4 mM of each deoxyribonucleotide triphosphates (dNTP) and 3.2 mM magnesium sulfate), 1 µl of reverse transcriptase/Taq mixture from the kit, 0.4 µl of a 50 mM magnesium sulfate solution, and 1 µg of nonacetylated bovine serum albumin (Roche). All used oligonucleotides were prepared and supplied by Tib-Molbiol, Berlin. To ensure reverse transcription, thermal cycling was maintained for 10 min at 55 °C, then for 3 min at 95 °C followed by 45 cycles of 95 °C for 15 s and 58 °C for 30 s. *In vitro* amplification of PCR target transcript regions was carried out and standard curves for quantitative evaluation of the viral RNA were prepared.

3. Results and discussion

3.1. Binding affinity analysis for proteins and ligands with molecular docking

To predict the antiviral activity of the components of the Egyptian propolis on a structural basis, automated docking studies were carried out using Molsoft ICM 3.4-8C program (https://www.rcsb.org/) the scoring functions and hydrogen bonds formed with the surrounding amino acids found in COVID-19 main protease and spike protein sequences are used to predict their binding modes, their binding affinities and orientation of these compounds at the active site of the single-crystal structures are available through the RCSB Protein Data Bank (PDB entries 6LU7, 7BZ5 respectively). The scoring functions of the compounds were calculated from minimized ligand-enzyme complexes.

3.2. Binding with COVID 3CL-protease

The 3CL-protease (main protease or M^pro) in COVID is essential for the proteolytic maturation of the virus and has been examined as a potential target protein to prevent the spread of infection by inhibiting the cleavage of the viral polyprotein (Abagyan and Totrov, 1994). The discovery of the 3CL-protease structure in COVID-19 provides a great opportunity to identify potential drug candidates for treatment. Proteases represent potential targets for the inhibition of COVID replication. The 3CL-protease amino acids Thr24, Thr26, and Asn119 (Verma et al.,

Table 2
ICM score, no. of H-bonds and amino acid residues involved in the interaction between components of Egyptian propolis, Remdesivir, Avigan, Hydroxychloroquine and N3, native ligand and the active site of COVID-19 3CL-protease.

Amino acid residues involved	No. of H-Bonds	ICM Score with COVID-19 M. protease	Comp.
GLY71, LYS97, GLY11, GLU14	5	−133.6	N3
GLN110, THR111, THR292, PHE294, ASP153, SER158.	10	−136.4	Remdesivir
GLN110, THR111, THR292, ASN151, ASP295.	6	−33.3	Avigan
GLN110, THR111, THR292.	3	−65.9	Hydroxychloroquine
LYS102, GLN110, ASN151, SER158, THR111, ILE152, ASP153	18	−92.8	Rutin
LYS102, ASP153.	5	−67.8	Caffeic acid phenethyl ester
LYS102, GLN110, THR111, ASP153, ASP295	10	−57.5	Quercetin
LYS5, LYS137, TYR239, GLU288, GLU290.	7	−56.3	Kaempferol
GLY71, N119, SER121.	3	−56.2	Pinocembrin
GLN110, THR111, SER158.	5	−54.1	Pinobanksin
GLY71, GLU14, GLY15, SER121.	4	−53.2	Galangin
LYS102, GLN110, THR111, S158, ASP295	8	−52.9	Chrysin
THR111, THR292, SER158.	5	−45.5	p-Cumaric acid
GLN110, THR111.	4	−35.4	Benzoic acid

2020). N3, the native ligand binds to amino acid residues PHE140, ASN142, GLU166, HIS163, HIS172, HIS41, MET49, TYR54, MET165, ASP187. MET165, LEU167, PHE185, GLN192, GLN189, PRO168, THR190, ALA191, THR24 and THR25 at the active site of main protease (Liu and Wang, 2020; Wan et al., 2020). Other amino acid residues as LYS102, GLN110, THR111, ASP295, ASN151, ILE152, ASP153, SER158, PHE294, THR292, are participating in the interaction at the binding pocket of 6LU7 to FDA approved antiviral compounds and active phytochemicals (Chandel et al., 2020; Dayer, 2020; Liu and Wang, 2020). In this study 14 compounds have been docked into the active site of COVID-19 3CL-protease. Ten of them are components of Egyptian propolis (Rutin, Caffeic acid phenethyl ester, Quercetin, Kaempferol, Pinocembrin, Pinobanksin, Galangin, Chrysin, p-Cumaric acid and Benzoic acid). N3, the native ligand of 6lu7, along with two clinically used drugs for treatment of COVID-19 infection (Avigan and hydroxyquinone (HQ)) and Remdesivir as a potential antiviral drug, were also applied for molecular docking. Results show that N3 reveals ICM score (Internal Coordinate Mechanics) of −133.56 and form 5H-bonds with amino acids GLY71, LYS97, GLY11, GLU14. Rutin shows ICM score of −92.78 and forms 18H-bonds with LYS102, GLN110, ASN151, SER158, THR111, ILE152, ASP153. Caffeic acid phenethyl ester shows much less ICM score than rutin, −67.81 and forms 5H-bonds with LYS102 and ASP153. Quercetin which shows relatively low ICM score of −57.48 forms 10*H*-bonds with LYS102, GLN110, THR111, ASP153, ASP295. Kaempferol ICM score is −56.26, it forms 7H-bonds with LYS5, LYS137, Y239, GLU288, GLU290. Pinocembrin shows ICM score of −56.21 and form 3H-bonds with GLY71, ASN119, SER121 while Pinobanksin ICM score was −54.08 and forms 5H-bonds with GLN110, THR111 and SER158. Galangin shows ICM score of −53.23 and 4H-bonds with GLY71, GLU14, GLY15 and SER121. Chrysin ICM score is −52.95 and forms 8 H-bonds with LYS102, GLN110, THR111, SER158, ASP295
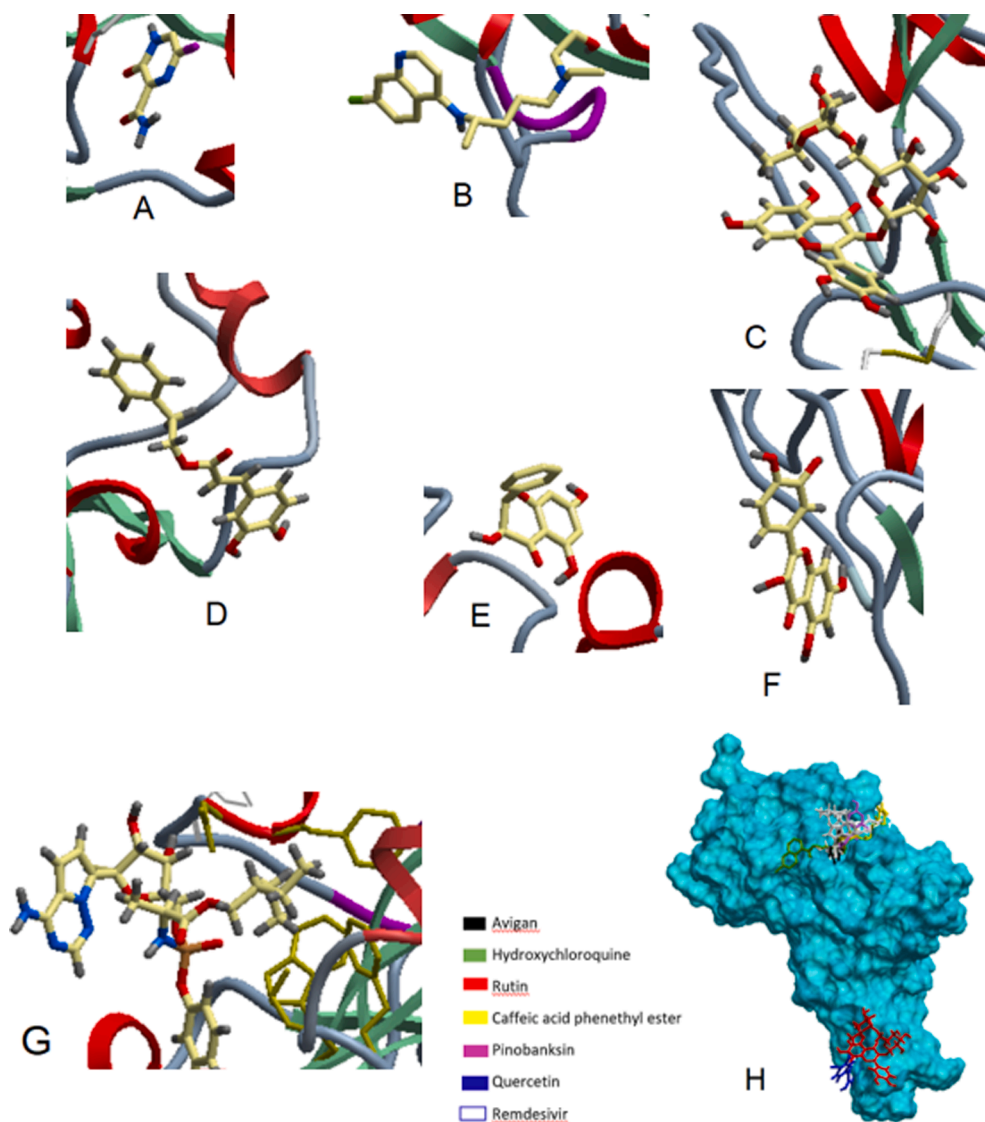
Fig. 2. 3D-plots for docking of A) Avigan; B) Hydroxychloroquine; C) Rutin; D) Caffeic acid phenethyl ester E) Pinobanksin and F) Quercetin G) Remdesivir in the active site of COVID-19 S1 spike protein, (pdb ID: 7BZ5). H) represents 3D-plot for comparison pose docking of 2 standards and the most active 4 components of Egyptian propolis.

Table 3

ICM score, no. of H-bonds and amino acid residues involved in the interaction between components of Egyptian propolis, Remdesivir, Avigan and hydroxychloroquine and active site of S1 spike protein of COVID-19:

Amino acid residues involved	No. of H-Bonds	ICM Score with Spike Protein	Comp.
ARG509, ASN343, ALA344	3	−165.9	Remdesivir
ARG509	3	−46.3	Avigan
TRP436, THR345	2	−79.8	Hydroxychloroquine
GLU484	1	−94.3	Rutin
ASN437, ALA372	2	−77.8	Caffeic acid phenethyl ester
TRP436, PHE342	3	−77.4	Pinobanksin
GLN474	2	−67.8	Quercetin
ASN343	1	−66.2	Chrysin
TRP436	2	−62.3	Kaempferol
GLY482	1	−60.5	Pinocembrin
GLY482	1	−59.5	Galangin
ARG509, SER373	3	−56.5	p-cumaric acid
TRP436	1	−40.4	Benzoic acid

Table 4

17 formulations and their responses values according to RSM.

Run	A: LMC	B: CH %	C: DL	E.E %	Release %
1	40	66	3.3	50.5 ± 1.3	27.5 ± 2.3
2	60	43	3.3	55.7 ± 2.2	72.5 ± 3.1
3	80	20	3.3	58.4 ± 1.6	84.2 ± 1.7
4	60	20	5	69.3 ± 2.1	80.3 ± 2.1
5	40	43	5	53.4 ± 1.9	60.2 ± 2.5
6	80	43	5	79.2 ± 0.9	73.6 ± 1.9
7	40	20	3.2	53.4 ± 1.1	77.5 ± 2.7
8	60	20	1.5	41.7 ± 1.7	75.6 ± 1.6
9	60	66	5	66 ± 2.2	30.8 ± 1.2
10	80	43	1.5	43 ± 1.1	70.95 ± 2.8
11	80	66	3.25	70.2 ± 2.3	29.8 ± 2.2
12	40	43	1.5	35 ± 1.7	53.6 ± 2.5
13	60	66	1.5	49.7 ± 2.8	29.5 ± 1.7
14	60	43	3.25	51 ± 2.9	60.5 ± 7.1
15	60	43	3.25	56.3 ± 1.5	77.99 ± 3.1
16	60	43	3.25	60 ± 1.7	72 ± 4.9
17	60	43	3.25	55.9 ± 1.8	71.5 ± 3.9

LMC: lipid molar concentration, CH%: cholesterol percentage, DL: drug loading.

whereas P-cumaric acid and benzoic acid reveals the lowest ICM scores of -45.50 with 5H-bonds with THR111, THR292 and SER158 and -35.43 with 4H-bonds with LYS110 and THR111, respectively (Fig. 1, Table 2).

The descending role of affinity to COVID-19 main protease is: Rutin > Caffeic acid phenethyl ester > Quercetin > Kaempferol > Pinobanksin > Galangin > Chrysin > p-cumaric acid > Benzoic acid. On comparison of these components of Egyptian propolis with Avigan, it is obviously observed that all propolis components have higher binding affinity than Avigan. Interestingly, Rutin has showed higher affinity than HQ. Moreover, Rutin showed a perspective binding affinity comparable to the potent antiviral drug, Remdesivir.

3.3. Binding with S1 spike protein of COVID-19

The spike protein, S protein, is a class I fusion protein. Each S protomer consists of S1 and S2 domains with the receptor binding domain (RBD) located on the S1 domain (Narkhede et al., 2020). S1 domain amino acid extended from 1 to 745 where (RBD) located in it extended from 375 to 604 (Han et al., 2017). Amino acid residues of the SARS-CoV-2 RBD LYS417, GLY446, TYR449, TYR453, LEU455, PHE456, ALA475, PHE486, ASN487, LYS489, GLN493, GLY496, GLN498, THR500, ASN501, GLY502 and LYS505 Are the residues in contact to ACE2 (Lan et al., 2020). On the other hand, amino acid residues in Contact between COVID-19 virus RBD and both heavy and light chains of B38 are reported (Jin et al., 2020). In this study, we docked certain components of Egyptian propolis, Avigan, hydroxychloroquine and

The descending role of affinity to S1 spike protein is: Remdesivir > Rutin > HCQ > Caffeic acid phenethyl ester > Pinobanksin > Quercetin > Chrysin > Kaempferol > Pinocembrin > Galangin > p-cumaric acid > Avigan > Benzoic acid.

3.4. Preparation of PP-Lip and optimization using RSM (response surface methodology)

The spraying technique has successfully produced a nanosized uniform PP-Lip, with the least aggregation of free unencapsulated propolis during preparation and with high propolis entrapment and release percentage mostly above 50% for both entrapped and release percentage (Table 4).

The effect of the three nominated factors was studied to optimize the formulation parameters for high entrapped and released flavonoidal content. The E.E% and released % were estimated for the 17 runs as the average of three replicates for each run and the results were provided in table 4.

Design expert software was used to analyze the measured data and the equations of regression were produced as follows:

$$Y_F = X_o + X_1 A + X_2 B + X_1 X_1 A_1 A_1 + X_2 X_2 B_2 B_2$$

Where Y_F represents the independent variable, X_o is the response of the arithmetic mean of the seventeen runs, and X_1 is the assessed coefficient factor for A. The average produced by changing a dependent variable once is represented by A and B. Non-linearity is estimated using $A_1 A_1$ and $B_2 B_2$. The magnitude and the sign of coefficients show the

$$E.E\% = +55.78 + 7.31A + 1.70B + 12.31C + 3.67AB + 4.45AC - 2.82BC - 0.8400A^2 + 3.18B^2 - 2.29C^2$$

$$Release = 70.91 + 4.96A - 25.00B + 1.90C - 1.0AB - 0.9775AC - 0.8475BC - 2.81A^2 - 13.35B^2 - 3.50C^2$$

Remdesivir into the active site of S1 spike protein of COVID-19 (Fig. 2, Table 3). Hydroxychloroquine reveals ICM score of -79.75 and form 2H-bond with TRP436, THR345. Remdesivir shows ICM score of -165.91 and form 3H-bond with ARG509, ASN343, ALA344 whereas Rutin which shows higher ICM score of -94.29 and forms only one H-bond with GLU484. While both CAPE and Pinobanksin show ICM score comparable to HQ of -77.82; 2H-bonds with ASN437 and ALA372 and -77.43; 3H-bond with TRP436 and PHE342, respectively. Quercetin and Chrysin show ICM score of -67.81; form 2H-bonds with GLN474 and -66.23; form one H-bonds with ASN343. Kaempferol ICM score is -62.33 and forms 2H-bonds with TRP436. Both Pinocembrin and Galangin reveal comparable ICM score of -60.46 and -59.47 respectively

impact of the three independent variables on the different responses.

3.5. Effect of each variable on the E.E %

The E.E % of prepared PP-Lip ranges between $35 \pm 1.73\%$ and $79.2 \pm 0.9\%$. The highest E.E % was achieved in run no.6 at which the Maximum level of LMC and DL were used with moderate CH%. The effect of LMC, CH% and DL on propolis E.E % was readily investigated.

$$E.E\% = +55.78 + 7.31A + 1.70B + 12.31C + 3.67AB + 4.45AC - 2.82BC - 0.8400A^2 + 3.18B^2 - 2.29C^2$$

and each one form only one H-bond with GLY482. ICM score of p-cumaric acid comes after that with the value of -56.53; forms 3H-bond with ARG509 and SER373. Finally, Benzoic acid shows the least affinity with ICM score of -40.40 and forms one H-bond with TRP436.

The verified model for E.E % is:

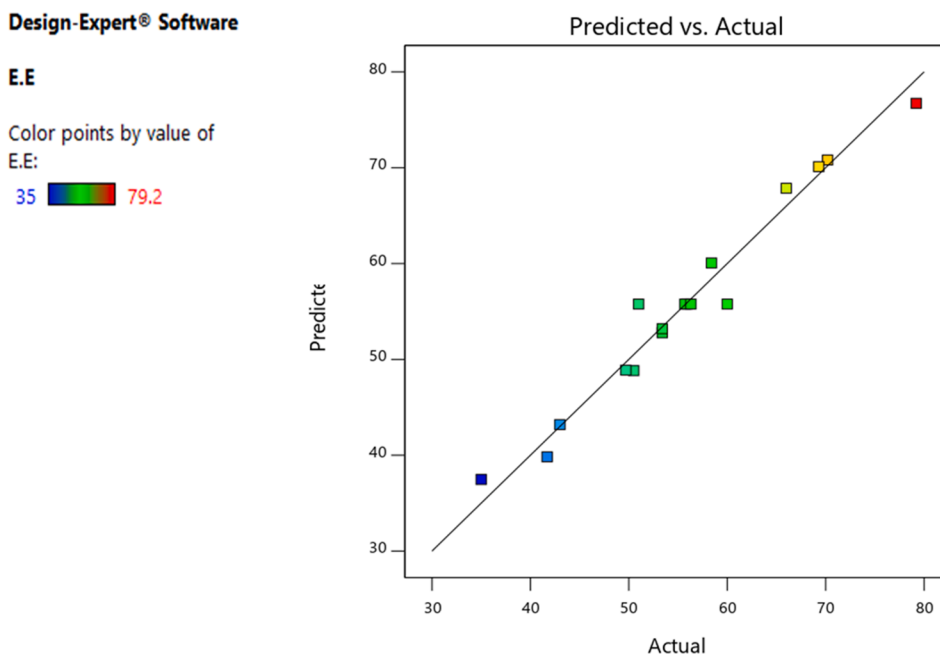It is clear from the obtained results that E.E % increases significantly

Fig. 3. predicted vs actual plot of the predicted model of the E.E %

from $35 \pm 1.73\%$ up to $79.2 \pm 0.9\%$ (P < 0.0001) with increasing LMC and DL (Table 4). The suggested model shows high correspondence between the predicted values and the actual experimental values (Fig. 3). This ensures the significance of the model and efficiency of the equation to predict the E.E % within the factors' levels used in the experiments. The correlation coefficient (R^2) shows that the predicted values and the actual data are significantly similar. The calculated values of R^2, $R^2_{Adj.}$ and $R^2_{Pred.}$ for the predicted E.E% model were 0.9654, 0.9209 and 0.748, respectively. The ANOVA of the quadratic model (Table 5) confirms that LMC and DL are highly significant model terms with positive sign (increasing these factors would increase the E.E %). On the other hand, CH% had insignificant effect on the E.E %. It is also noticeable that there was an interaction between LMC and DL where increasing both factors increases the value of the E.E %. Table 5 shows that ANOVA of model of regression for the E.E% of PP-Lip was estimated by F-test and p-value. The highly significant p-value (P = 0.0003) and the p-value of lack-of-fit which is greater than 0.05 (0.5248) indicate the capability of the fitted regression equation in justifying and expecting the results.

Data obtained from the ANOVA was confirmed by studying the effect of each factor on the E.E % (Fig. 4). It is obvious that the results of individual effect of each factor confirmed the positive effect of LMC and DL on E.E%.

The positive significant interaction between LMC and DL shown by ANOVA was confirmed by the interaction plot (Fig. 5). The interaction plot showed slight increase in E.E% on increasing the LMC at lower level of DL (1.5 mg/ml). On the other hand, there was a significant increase in the E.E % on increasing LMC at higher level of DL (5 mg/ml). This observation was also evident in the 3D plot of E.E % and its relationship with LMC and DL (Fig. 6) where E.E % reached to higher values at maximum levels of LMC and DL. this is in consistence with *Mostafa et al* (Mostafa et al., 2018) who stated the increased E.E% of thymoquinone due to increased LMC. This could be attributed to increased width of lipid bilayer membrane. Interestingly, *Arafa et al* (Arafa et al., 2018) stated the increased E.E% of propolis with increased DL which could be attributed to the enhanced capacity of the prepared nanostructure. Unlikely, Results showed that CH% had no effect on E.E % of the prepared PP-Lip. This was in contrast with *Mclntosh et al* (McIntosh, 1978) who stated that increasing CH% leads to increased E.E % due to increased particle size and width of the prepared liposomes to entrap more drug. This discrepancy may be due the small particle size of the prepared PP-Lip prepared by modified spraying technique.

3.6. Effect of each variable on the release %

Table 4 shows the results of the release study for the 17 formulations. The release % of prepared PP-Lip ranged between $27.5 \pm 2.3\%$ and $84.15 \pm 1.17\%$. The highest release was achieved in run 3 at which the Maximum level of LMC, moderate level of DL and minimum level of CH % were maintained.

The equation that represents the release % model was generated by desgin expert software as follow:

Release % = $70.91 + 4.96$ A $- 25.00$B $+ 1.90$C $- 1.0$ AB $- 0.9775$ AC $- 0.8475$ BCE $- 2.81$ A^2 $- 13.35$ B^2 $- 3.50$ C^2

The suggested model revealed high similarity between the predicted values and the actual experimental data (Fig. 7). This emphasizes the significance of the model and efficiency of the equation to predict the release % within the factors' levels used in the experiments. ANOVA of
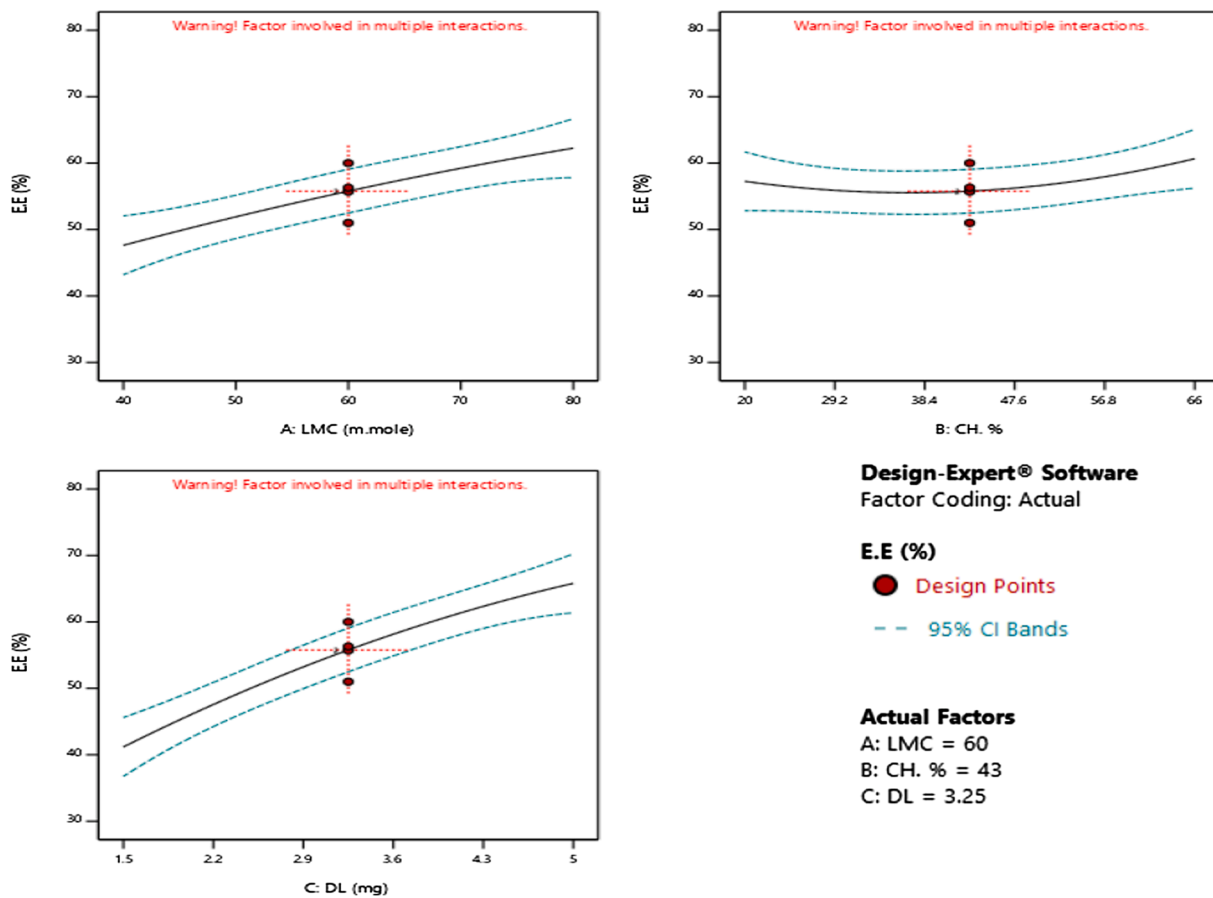
Table 5
ANOVA of the E.E % predicted model.

Source	Sum of Squares	Df	Mean Square	F-value	p-value	Significance
Model	1893.2	9	210.4	21.7	0.0003	S
A-LMC	427.8	1	427.8	44.2	0.0003	S
B-Ch. %	23.1	1	23.1	2.4	0.17	NS
C-DL	1212.8	1	1212.8	125.2	< 0.0001	S
AB	54.02	1	54.02	5.6	0.05	NS
AC	79.2	1	79.2	8.2	0.02	S
BC	31.9	1	31.9	3.3	0.1	NS
A^2	2.97	1	2.97	0.30	0.6	NS
B^2	42.7	1	42.7	4.4	0.07	NS
C^2	22.08	1	22.1	2.3	0.17	NS
Residual	67.8	7	9.7			
Lack of Fit	26.9	3	8.9	0.9	0.5	NS
Pure Error	40.9	4	10.2			
Cor Total	1961.03	16				

HS: highly significant, S: significant and NS: not significant.
$R^2 = 0.9654$ $R^2_{Adj.} = 0.9209$ $R^2_{Pred.} = 0.748$

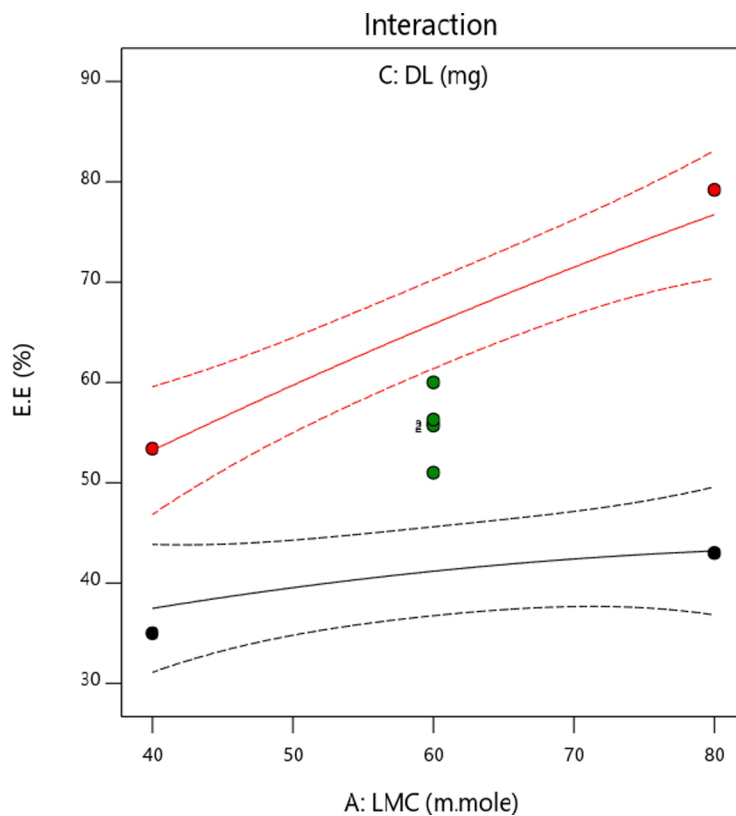**Fig. 4.** Effect of LMC, CH% and DL on E.E % of PP-Lip.

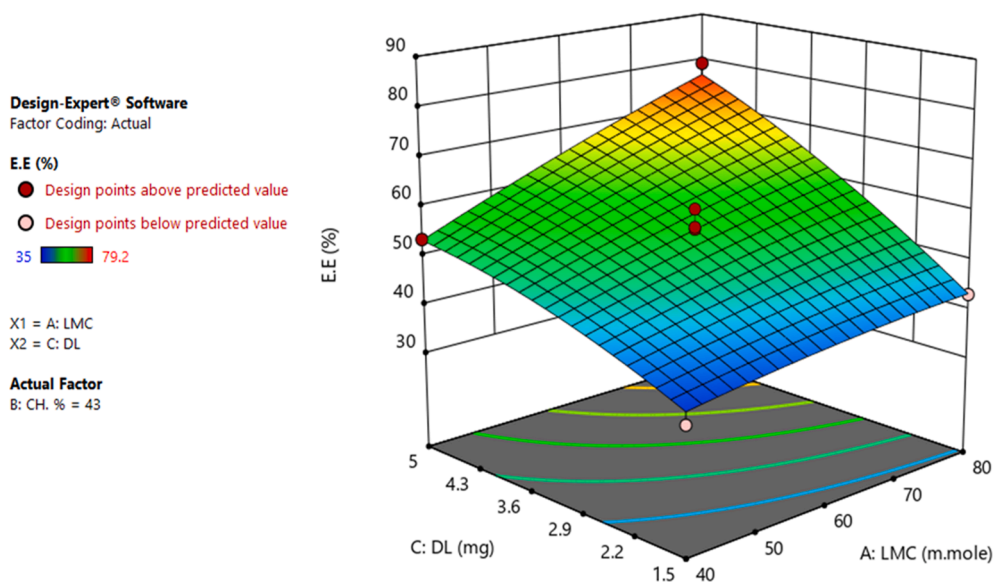**Fig. 5.** Interactive effect of LMC and DL on E.E %

Fig. 6. 3D surface plot of E.E % model.

regression model for the release % of PP-Lip revealed a highly significant p-value, P = 0.0003 (Table 5). The p-value of lack-of-fit was greater than 0.05 (0.6627) indicating that the equation of the fitted regression was good and capable of elucidating and expecting the results. Results show that CH% (B) has a dramatic significant negative effect on release unlike LMC (A) which has a slight positive effect on release % while DL has no effect on the release % (Table 4, Fig. 8). The 3D plot (Fig. 9) approves the effect of the LMC and CH% on release %. At LMC 40 mM, increasing the CH% from 20% to 66% decreases the release % significantly from 77.5 ± 2.73 to 27.5 ± 2.3, respectively. At CH% equals 20%, the release % shows the highest values with varying LMC. The slight positive effect of LMC a on release % may be attributed to the enhanced engagement of

the lipid bilayer to the structurally similar cell membrane. Increasing Cholesterol % has resulted in lower release % which could be attributed increasing the rigidity and decreasing the fluidity of the lipid bilayer (Gier et al., 1969; Niven and Schreier, 1990). Reduction of cholesterol concentration makes the liposomes more fluid enhancing the drug release and so drug pharmacological effects (A Ghaffar et al., 2016).

3.7. Optimization of formulation paramaters to achieve the highest E.E% and release %.

The preparation conditions were set in the box-behnken design to formulate PP-Lip with the highest E.E% and release %. The optimized
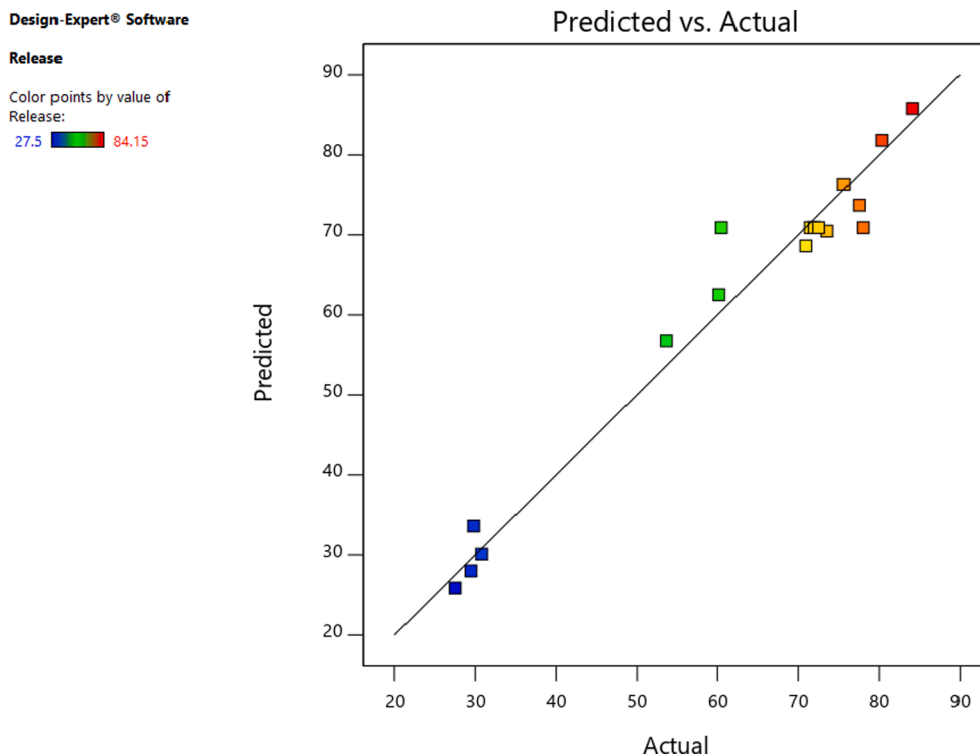

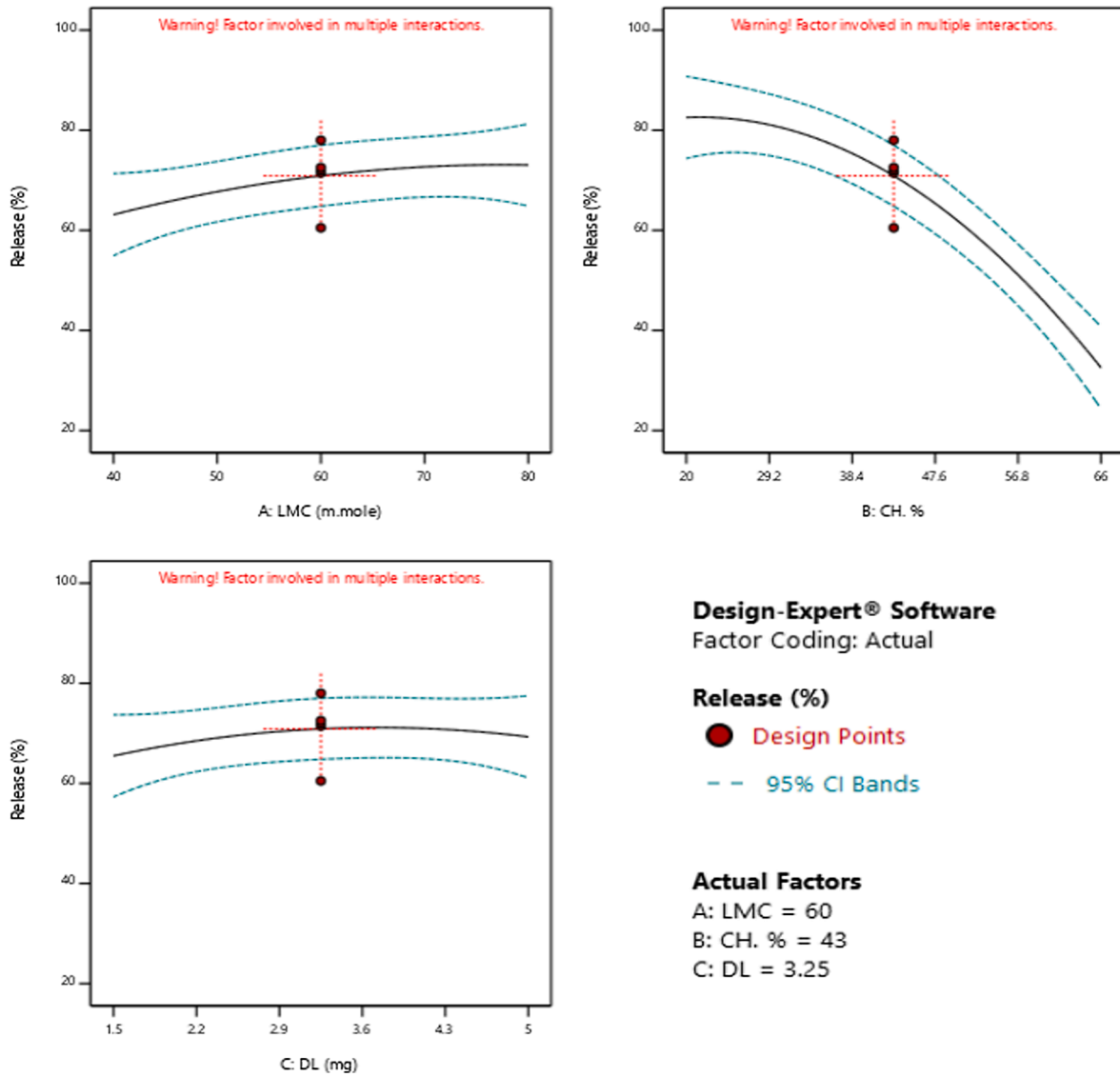**Fig. 7.** Predicted vs actual plot of suggested model of release %.
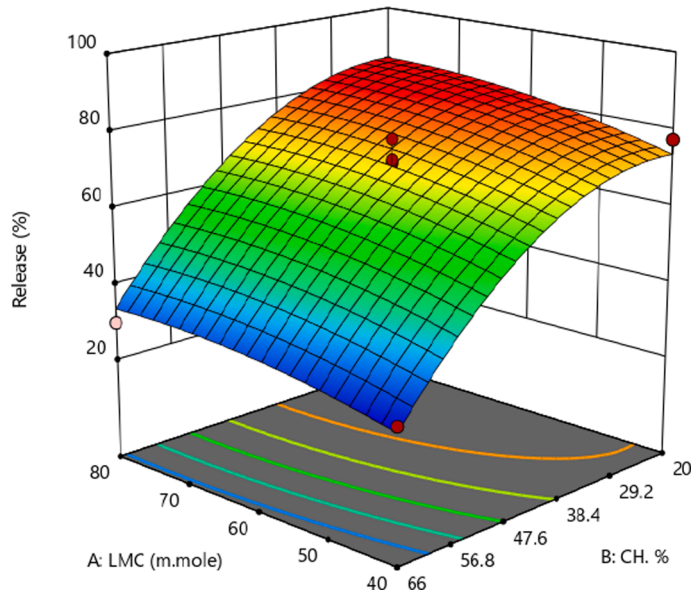
Fig. 8. Effect of LMC, CH% and DL on release % of PP-Lip.

Fig. 9. 3D surface plot of the release model.
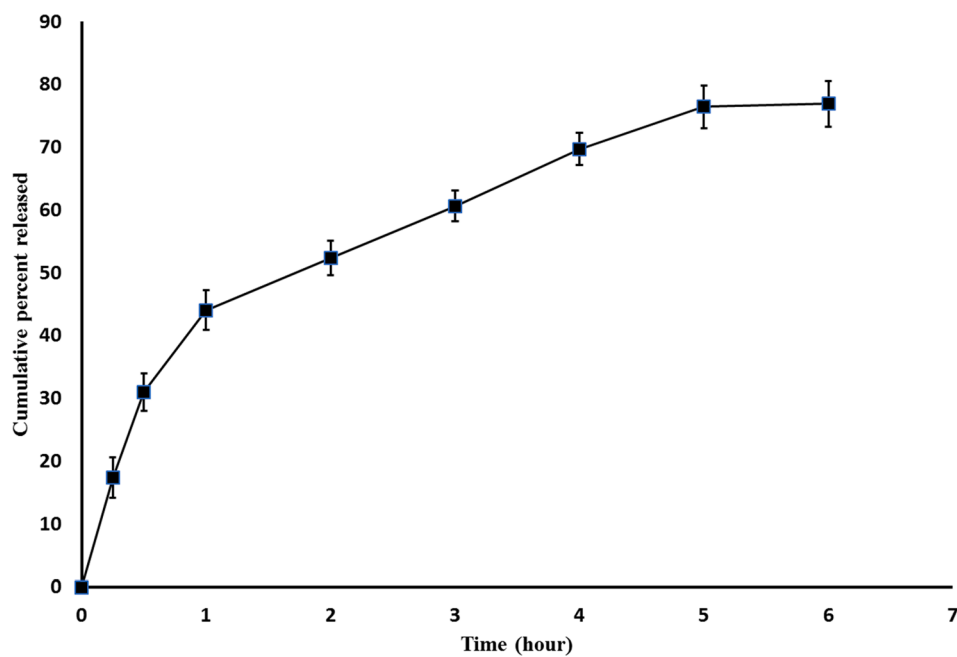
Fig. 10. Cumulative % released from optimized liposomal formulation.

80-100-1.tif
Print Mag: 72100x @ 86 mm
11:09 10/10/19

100 nm

HV=80.0kV
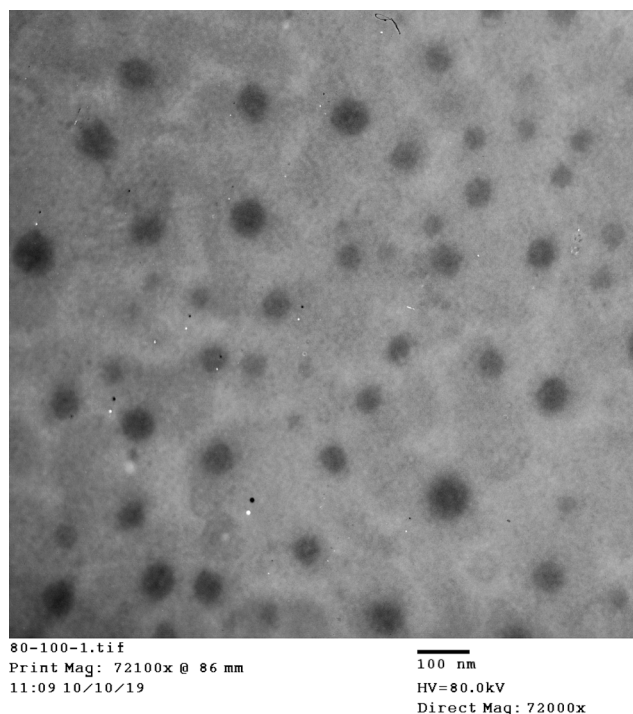Direct Mag: 72000x

Fig. 11. TEM of optimized propolis liposomes.

formulation parameters were as follow: LMC of 60 m.mole, CH% of 20% and DL of 5 mg/ml. At those values the E.E% and released % were 70.112% and 81.801%, respectively. Five verification experiments were carried out at these optimium conditions to ensure the model capablility to optimize the conditons as directed. The E.E% and released % were 68 $\pm$ 2.4% and 76 $\pm$ 3.2%, respectively (Fig. 10). Release pattern follows the 1st order kinetics with R^2 0.992. Furthermore, the Particle size of the optimized PP-Lip was 117 $\pm$ 11 nm (Fig. 11). These results indicate that the optimization process is successful in practical lab work.

3.8. In vitro 3CL-protease inhbition

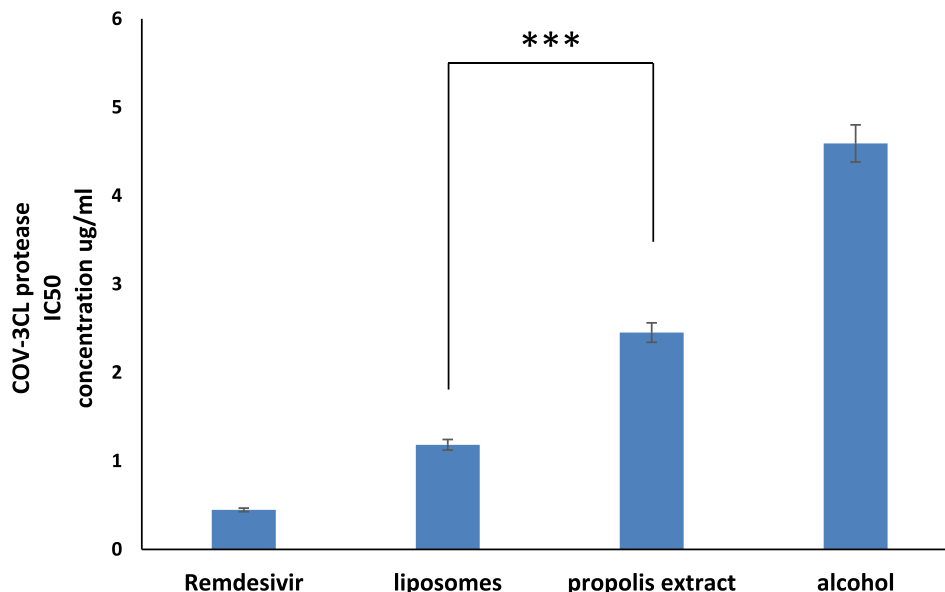3CL protease has been an important target for the prevention of the

replication of corona virus especially that it has not been found in hostcells (Akaji et al., 2011). Results show that propolis extract possess a good inhibitory effect against covid-3CL-protease (IC50 = 2.452 $\pm$ 0.11) (Fig. 12). That could be justified by binding of the studied propolis-flavonoids to the active site of 3CL- protease. Competitive inhibition of the protease resulted from strong binding to such flavonoids could result in blocking the enzyme activity (Pillaiyar et al., 2016). Fortunately, that inhibitory effect was significantly enhanced via the encapsulation of the extract within the optimized liposomal formulation (IC50 = 1.183 $\pm$ 0.06), P < 0.001. We believe that the prepared liposomal system had the potential to flawlessly introduce both the hydrophilic and the lipophilic components of the extract via an enhanced surfaced surface area with avoiding the sticky nature of the extract.

3.9. Anti-viral effect using RT-PCR

To gain more insight into the effect of the formulation of the propolis extract on the enhancement of the anti-viral effect on COVID-19 virus, viral replication was determined using RT-PCR. Results show the great impact of the optimized propolis liposomal formulation in enhancing the inihbitory effect of the encasulated propolis against covid viral replication compared to the unformulated propolis extract (87.9 $\pm$ 1.2, 72.4 $\pm$ 0.5, respectively) (P < 0.0001). We suppose that encapsulation of propolis within an optimized liposomal system would enhance cell permeability of propolis components due to increased surface area available for endocytosis and the silmilarity of lipid structure of the liposomal membrane to cell membrane. Moreover, the liposomal system is capable of introducing both the hydrophilic and the lipophilic components of propolis for cellular uptake avoiding retaining of lipophilic components within the liposomal mebrane and/or poor cellular uptake of the hydrophilic components of propolis extract.

Interestnigly, the optimized propolis liposomes has comparatively inhibited the replication of human corona virus such as remedsivir, antiviral drug with reported promising *in vitro* inhibitory effect on covoid-19 (Hashemian et al., 2020) (87.9 $\pm$ 1.2, 91.2 $\pm$ 2.5, respectively), Fig. 13.

4. Conclusion

The present study has revealed the anti-viral potential of flavonoidal components of Egyptian propolis. Molecular docking has shown that all propolis components have high binding affinity to COVID 3-CL protease
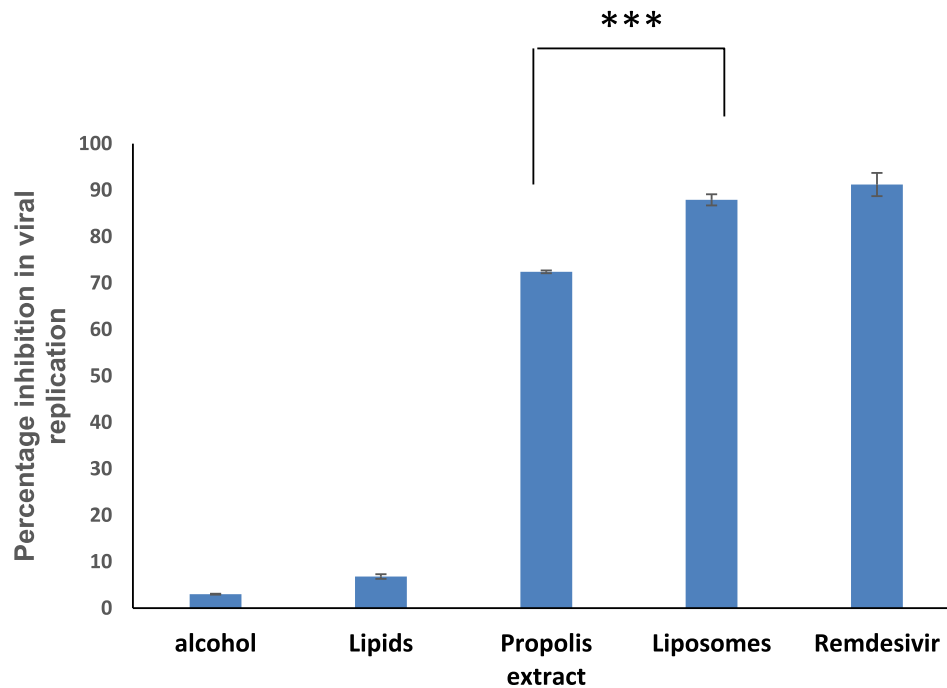

Fig. 12. *In vitro* 3CL-protease inhibition.

Fig. 13. Inhibition of viral replication by Propolis extract, alcohol, propolis liposomes and control.

and spike protein compared to Avigan, hydroxychloroquine (HQ) and Remdesivir. An optimized liposomal formulation could guarantee both the enhanced delivery to the target cells and the improved cellular uptake of encapsulated propolis. To the best of our knowledge, that has been the first study that estimates the effect of a nanocarrier dosage form on the enhancement of the anti-viral effect of Egyptian propolis extract against Covid-19. Further clinical studies are being carried out to estimate the effeciency of the optimized formulation against COVID-19.

Funding

This research did not receive any specific grant from funding agencies in the public, commercial, ornot-for-profit sectors.

Declaration of Competing Interest

The authors declare that they have no known competing financial interests or personal relationships that could have appeared to influence the work reported in this paper.

References

Ghaffar, K., Marasini, N., Giddam, A., Batzloff, M., Good, M., Skwarczynski, M., Toth, I., 2016. The Role of Size in Development of Mucosal Liposome-Lipopeptide Vaccine Candidates Against Group A Streptococcus. MC 13 (1), 22–27.

Abagyan, R., Totrov, M., 1994. Biased Probability Monte Carlo Conformational Searches and Electrostatic Calculations for Peptides and Proteins. Journal of Molecular Biology 235 (3), 983–1002.

Akaji, K., Konno, H., Mitsui, H., Teruya, K., Shimamoto, Y., Hattori, Y., Ozaki, T., Kusunoki, M., Sanjoh, A., 2011. Structure-Based Design, Synthesis, and Evaluation of Peptide-Mimetic SARS 3CL Protease Inhibitors. J. Med. Chem. 54 (23), 7962–7973.

Arafa, M.G., Ghalwash, D., El-Kersh, D.M., Elmazar, M., 2018. Propolis-based niosomes as oromuco-adhesive films: A randomized clinical trial of a therapeutic drug delivery platform for the treatment of oral recurrent aphthous ulcers. Scientific reports 8 (1), 18056.

Badria, F., Fathy, H., Fatehe, A., Ahmed, M., Ghazy, M., 2018. Chemical and biological diversity of propolis samples from Bulgaria, Libya and Egypt. J Apither 4 (1), 17. https://doi.org/10.5455/ja.10.5455/ja.20180428014109.

Banskota, A.H., Tezuka, Y., Kadota, S., 2001. Recent progress in pharmacological research of propolis. Phytother. Res. 15 (7), 561–571.

Chandel, V., S. Raj, B. Rathi, D. Kumar, 2020. In Silico Identification of Potent COVID-19 Main Protease Inhibitors from FDA Approved Antiviral Compounds and Active Phytochemicals through Molecular Docking: A Drug Repurposing Approach.

Dayer, M. R., 2020. Old drugs for newly emerging viral disease, COVID-19: Bioinformatic Prospective. arXiv preprint arXiv:2003.04524.

Drosten, C., Günther, S., Preiser, W., van der Werf, S., Brodt, H.-R., Becker, S., Rabenau, H., Panning, M., Kolesnikova, L., Fouchier, R.A.M., Berger, A., Burguière, A.-M., Cinatl, J., Eickmann, M., Escriou, N., Grywna, K., Kramme, S., Manuguerra, J.-C., Müller, S., Rickerts, V., Stürmer, M., Vieth, S., Klenk, H.-D., Osterhaus, A.D.M.E., Schmitz, H., Doerr, H.W., 2003. Identification of a Novel Coronavirus in Patients with Severe Acute Respiratory Syndrome. N Engl J Med 348 (20), 1967–1976.

El Hady, F.K.A., Hegazi, A.G., 2002. Egyptian propolis: 2. Chemical composition, antiviral and antimicrobial activities of East Nile Delta propolis. Zeitschrift für Naturforschung C 57 (3–4), 386–394.

Fueldner, H.H., 1981. Characterization of a third phase transition in multilamellar dipalmitoyllecithin liposomes. Biochemistry 20 (20), 5707–5710.

De Gier, J., Mandersloot, J.G., Van Deenen, L.L.M., 1969. The role of cholesterol in lipid membranes. Biochimica et Biophysica Acta (BBA) - Biomembranes 173 (1), 143–145.

Gordon, C.J., Tchesnokov, E.P., Feng, J.Y., Porter, D.P., Götte, M., 2020. The antiviral compound remdesivir potently inhibits RNA-dependent RNA polymerase from Middle East respiratory syndrome coronavirus. J. Biol. Chem. 295 (15), 4773–4779.

Güler, H. I., G. Tatar, O. Yildiz, A. O. Belduz and S. Kolayli, 2020. Investigation of potential inhibitor properties of ethanolic propolis extracts against ACE-II receptors for COVID-19 treatment by Molecular Docking Study. ScienceOpen Preprints.

Günther, S., Asper, M., Röser, C., Luna, L.K., Drosten, C., Becker-Ziaja, B., Borowski, P., Chen, H.-M., Hosmane, R.S., 2004. Application of real-time PCR for testing antiviral compounds against Lassa virus, SARS coronavirus and Ebola virus in vitro. Antiviral Research 63 (3), 209–215.

Han, X., Qi, J., Song, H., Wang, Q., Zhang, Y., Wu, Y., Lu, G., Yuen, K.-Y., Shi, Y., Gao, G. F., 2017. Structure of the S1 subunit C-terminal domain from bat-derived coronavirus HKU5 spike protein. Virology 507, 101–109.

Hashemian, S.M., Farhadi, T., Velayati, A.A., 2020. A Review on Remdesivir: A Possible Promising Agent for the Treatment of COVID-19. Drug design, development and therapy 14, 3215.

He, J., Hu, L., Huang, X., Wang, C., Zhang, Z., Wang, Y., Zhang, D., Ye, W., 2020. Potential of coronavirus 3C-like protease inhibitors for the development of new anti-SARS-CoV-2 drugs: Insights from structures of protease and inhibitors. International Journal of Antimicrobial Agents 106055.

https://www.rcsb.org/.

Jin, Z., Du, X., Xu, Y., Deng, Y., Liu, M., Zhao, Y., Zhang, B., Li, X., Zhang, L., Peng, C., 2020. Structure of M pro from SARS-CoV-2 and discovery of its inhibitors. Nature 1–5.

Kujumgiev, A., Tsvetkova, I., Serkedjieva, Yu., Bankova, V., Christov, R., Popov, S., 1999. Antibacterial, antifungal and antiviral activity of propolis of different geographic origin. Journal of Ethnopharmacology 64 (3), 235–240.

Kumazawa, S., Hamasaka, T., Nakayama, T., 2004. Antioxidant activity of propolis of various geographic origins. Food Chemistry 84 (3), 329–339.

Lan, J., Ge, J., Yu, J., Shan, S., Zhou, H., Fan, S., Zhang, Q.i., Shi, X., Wang, Q., Zhang, L., Wang, X., 2020. Structure of the SARS-CoV-2 spike receptor-binding domain bound to the ACE2 receptor. Nature 581 (7807), 215–220.

Lan, X.i., Wang, W., Li, Q., Wang, J., 2016. The Natural Flavonoid Pinocembrin: Molecular Targets and Potential Therapeutic Applications. Mol Neurobiol 53 (3), 1794–1801.

Liu, X., Wang, X.-J., 2020. Potential inhibitors against 2019-nCoV coronavirus M protease from clinically approved medicines. Journal of Genetics and Genomics 47 (2), 119.

Liu, Y., A. A. Gayle, A. Wilder-Smith and J. Rocklöv, 2020. The reproductive number of COVID-19 is higher compared to SARS coronavirus. Journal of travel medicine.

López-Pinto, J.M., González-Rodríguez, M.L., Rabasco, A.M., 2005. Effect of cholesterol and ethanol on dermal delivery from DPPC liposomes. International Journal of Pharmaceutics 298 (1), 1–12.

Marcucci, M.C., 1995. Propolis: chemical composition, biological properties and therapeutic activity. Apidologie 26 (2), 83–99.

Maruta, H., 2014. Herbal Therapeutics that Block the Oncogenic Kinase PAK1: A Practical Approach towards PAK1-dependent Diseases and Longevity: PAK1-blocking herbal therapeutics. Phytother. Res. 28 (5), 656–672.

Maruta, H., He, H., 2020. PAK1-blockers: Potential Therapeutics against COVID-19. Medicine Drug Discovery 100039.

McIntosh, T.J., 1978. The effect of cholesterol on the structure of phosphatidylcholine bilayers. Biochimica et Biophysica Acta (BBA) - Biomembranes 513 (1), 43–58.

Mostafa, M., Alaaeldin, E., Aly, U.F., Sarhan, H.A., 2018. Optimization and Characterization of Thymoquinone-Loaded Liposomes with Enhanced Topical Anti-inflammatory Activity. AAPS PharmSciTech 19 (8), 3490–3500.

Narkhede, R.R., Cheke, R.S., Ambhore, J.P., Shinde, S.D., 2020. The molecular docking study of potential drug candidates showing anti-COVID-19 activity by exploring of therapeutic targets of SARS-CoV-2. screening 5, 8.

Niven, R.W., Schreier, H., 1990. Nebulization of liposomes. I. Effects of lipid composition. Pharmaceutical research 7 (11), 1127–1133.

Pillaiyar, T., Manickam, M., Namasivayam, V., Hayashi, Y., Jung, S.-H., 2016. An Overview of Severe Acute Respiratory Syndrome–Coronavirus (SARS-CoV) 3CL Protease Inhibitors: Peptidomimetics and Small Molecule Chemotherapy. J. Med. Chem. 59 (14), 6595–6628.

Refaat, H., Naguib, Y.W., Elsayed, M., Sarhan, H.A., Alaaeldin, E., 2019. Modified spraying technique and response surface methodology for the preparation and optimization of propolis liposomes of enhanced anti-proliferative activity against human melanoma cell line A375. Pharmaceutics 11 (11), 558.

Simone-Finstrom, M., Spivak, M., 2010. Propolis and bee health: the natural history and significance of resin use by honey bees. Apidologie 41 (3), 295–311.

Tolba, M.F., Azab, S.S., Khalifa, A.E., Abdel-Rahman, S.Z., Abdel-Naim, A.B., 2013. Caffeic acid phenethyl ester, a promising component of propolis with a plethora of biological activities: A review on its anti-inflammatory, neuroprotective, hepatoprotective, and cardioprotective effects: CAPE biological activities. IUBMB Life 65 (8), 699–709.

Verma, D., S. Kapoor, S. Das and K. Thakur, 2020. "Potential inhibitors of SARS-CoV-2 Main protease (Mpro) identified from the library of FDA approved drugs using molecular docking studies.".

Wan, Y., Shang, J., Graham, R., Baric, R.S., Li, F., 2020. Receptor recognition by the novel coronavirus from Wuhan: an analysis based on decade-long structural studies of SARS coronavirus. Journal of virology 94 (7).

Woisky, R.G., Salatino, A., 1998. Analysis of propolis: some parameters and procedures for chemical quality control. Journal of Apicultural Research 37 (2), 99–105.

Wu, Y., Wang, F., Shen, C., Peng, W., Li, D., Zhao, C., Li, Z., Li, S., Bi, Y., Yang, Y., Gong, Y., Xiao, H., Fan, Z., Tan, S., Wu, G., Tan, W., Lu, X., Fan, C., Wang, Q., Liu, Y., Zhang, C., Qi, J., Gao, G.F., Gao, F., Liu, L., 2020. A noncompeting pair of human neutralizing antibodies block COVID-19 virus binding to its receptor ACE2. Science 368 (6496), 1274–1278.

Zhu, N.a., Zhang, D., Wang, W., Li, X., Yang, B.o., Song, J., Zhao, X., Huang, B., Shi, W., Lu, R., Niu, P., Zhan, F., Ma, X., Wang, D., Xu, W., Wu, G., Gao, G.F., Tan, W., 2020. A Novel Coronavirus from Patients with Pneumonia in China, 2019. N Engl J Med 382 (8), 727–733.